23rd International Congress on Sound & Vibration
Athens, Greece 10-14 July 2016
ICSV23

BOUNDARY LAYER INTERACTION WITH POROUS SURFACE AND IMPLICATIONS FOR AERODYNAMIC NOISE REDUCTION

Syamir A. Showkat Ali and M. Azarpeyvand
Department of Mechanical Engineering, University of Bristol, BS8 1TR, UK
email: ss14494@bristol.ac.uk

Carlos R. Ilário da Silva
Embraer, São José dos Campos, 12227-901, Brazil

The present study discusses the mechanisms of flow interaction with porous surfaces as a passive flow control method for blunt trailing edges. To better understand the effect of flow interaction with a porous surface, measurements have been carried out for the boundary layer growth and boundary layer surface pressure and velocity correlations. Hot-wire measurements are also performed to investigate the energy content of the turbulent structure within the boundary layer. Two types of porous materials are considered for this study. Results have shown that the use of porous materials can stabilize the boundary layer growth, lessen the surface pressure fluctuations and reduce the energy content of the large turbulent structure in the outer layer. These results are essential for understanding the flow-porous interaction in real world applications.

1. Introduction

The blunt trailing edge bodies have been widely used for numerous aerodynamic applications, such as the wind turbine blades. However, the use of blunt trailing edges results in structural vibration and increase of drag, which is due to the undesirable vortex shedding generated by the blunt trailing edge. Generally, in order to reduce the trailing edge noise and control the flow, several passive methods, such as serrations [1–5], morphing [6, 7], porous materials [8] and etc, have been investigated over the past decades. Porous treatments have been of much interest amongst the the other passive treatments.

The use of porous materials for blunt bodies to improve their aerodynamic and aeroacoustic performance has been the subject of numerous experimental and numerical research studies over the previous decades [9–13]. Blunt trailing edge noise has been an important topic due to the wide range of engineering applications they feature in. Interest in blunt airfoils, also called “thick airfoil” in several studies have shown significant improvement in the lift performance for a wide range of Reynolds number applications. Standish and Van Dam [9] showed that blunt airfoils generate steep adverse pressure gradients leading to the premature flow separation. This can be seen from the upper surface of the airfoil even with small perturbations which moves a portion of pressure recovery to the airfoil’s wake. Hoerner and Borst [10] showed that blunt trailing edge on symmetric G-490 airfoil have significant increase in the maximum lift coefficient and maximum-thickness to chord ratio (t/c) using a constant chord Reynolds number of 500,000.

The effect of porous treatment on blunt trailing edge of a flat plate have been investigated numerically by Bae *et al.* [11]. Bae and Moon [12] have studied the effects of permeable material surfaces on turbulent noise generated by a blunt trailing edge of flat plate using LES, and the results have

shown significant reduction of the broadband noise over a wide range of frequencies. Zhou *et al.* [13] developed a discrete adjoint-based optimization framework to obtain optimal distribution of porous material on trailing edge of a flat plate using an LES solver. The results obtained indicated that there is possibility of minimizing the turbulence near the trailing edge and therefore controlling the noise generation at the trailing edge.

As reviewed above, the viability of using porous materials as a passive method to control the flow and weaken aero-acoustic type noise sources has been verified experimentally and numerically in several research works over the past decades. In some more recent research activities, it has been tried to further improve the effectiveness of such porous treatments by optimizing the shape and mechanical properties of the porous section, *i.e.* porosity and resistivity. In this paper, passive flow control method based on porous material for blunt trailing edge has been investigated. The experimental setup and wind- tunnel tests are described in Sec. 2. The results and discussions are detailed in Sec. 3.

2. Measurement Setup

The experiments were performed in the open jet wind tunnel of University of Bristol (UoB) with two different porous materials applied at the blunt trailing edge. The wind tunnel has a diameter of 1 m diameter and with a test section length of 2 m. The maximum reliable speed is 30 m/s with a maximum turbulence intensity of 0.05 %. The model of the blunt trailing edge flat plate rig is shown in Fig. 1 (a). The plate has a fore-body length of L_x = 350 mm and spanwise length of 715 mm (L_z) and h =20 mm thickness. The model in the open jet wind tunnel gives a blockage ratio of $BR = 1.8$ %, which clearly has negligible effect on any obtained results [14]. The flat plate has an elliptical leading edge in order to prevent flow separation at the beginning of the plate, and to help for the turbulent boundary layer to develop before the porous region. In order to reach a well-developed turbulent flow before the porous section, a 25 mm wide sand trip was applied just after the leading edge with a thickness of approximately 0.6 mm and grit roughness of 80. The trip was placed on both sides of the plate. The porous section is placed at the trailing edge with a width (L_{px}) and length (L_{pz}) of 50 mm and 500 mm, respectively. Two different metal porous materials were used with 25 and 80 pores per inch (PPI), which were made of aluminium. To ensure two dimensional flow over the span rectangular side-plates (425 mm x 80 mm) with sharpened leading edges with an angle of 20° were mounted on the rig. The side-plates were installed approximately $1.25h$ from the leading edge and $2.5h$ from the trailing edge.

To measure the turbulent properties of the flow, the measurements were carried out using single and cross hot-wire probes. The single hot-wire probes were Dantec 55P16 type with a platinum-plated tungsten wire of 5 μ m diameter and 1.25 mm length. The cross hot-wire (X-wire) probe was a Dantec 55P51 type sensor with 5 μm diameter and 3 mm length platinum-plated tungsten wires. The probes were operated by a Dantec StramlinePro frame which has two CTA91C10 modules. The applied overheat ratio was 1.8. The signal was low-pass filtered by the StreamlinePro frame with a corner frequency of 30 kHz before it was A/D converted. The data was acquired by a National Instrument 9215 type device, with a sampling frequency of to 40 kHz. The signals of the hot-wires were measured for 15 seconds at each location. The calibration of the wires were performed using a Dantec 54H10 type calibrator. FG-23329-P07 miniature microphones are used for the measurement of the unsteady boundary layer surface pressure fluctuating. The microphones dimensions are of 2.5 mm diameter and height with 0.8 mm of circular sensing area. The trailing edge plate was instrumented with 6 microphones under a pinhole mask of 0.4 mm diameter in order to compensate the large discontinuities [15] of the pressure attenuation at the wall interfered with the turbulent field. Hence, a small-sized pinhole microphones sensing area can be used to minimize the pressure attenuation effect [16]. The microphones were installed inside the plate parallel (horizontally) to the surface and were arranged on the surface in the streamwise directions. The location of the microphones is summarized in Table 1. Extension of this test with different porosities and permeability constants,

over a wide range of Reynolds numbers will be further developed using a flat plate equipped with several static pressure taps, surface pressure microphones and hotfilm probes, see Fig. 1 (b).

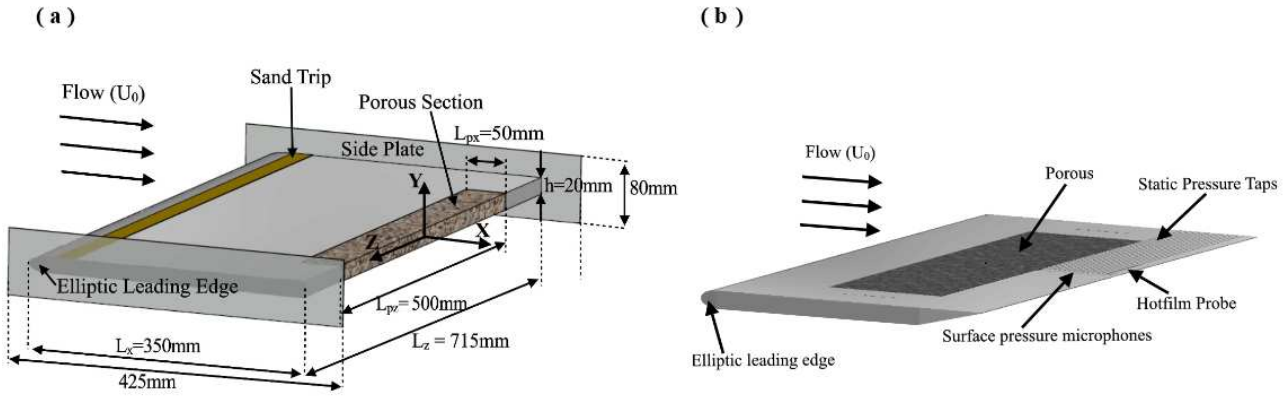

Figure 1: Design configuration (a) Flat plate blunt trailing edge schematic and (b) Flat plate design for future study

Table 1: Positions of pinholes microphones on the trailing edge

Position	Microphones Number	Distance from Trailing Edge (mm)	Distance from Mid Span (mm)
Streamwise	1, 2, 3, 4, 5, 6	7, 14, 20, 26, 32, 38	0.0

3. Results and Discussion

To better understand the effect of porous trailing edge on the aerodynamic performance and noise reduction, the boundary layer velocity profile and their energy content are presented in this section. Further discussions on the velocity-pressure correlation in the boundary layer is also be presented.

3.1 Velocity Profile and Their Energy Content

The behaviour of the boundary layer upstream of the blunt trailing edge was studied for different cases. The measurement is conducted at zero angle of attack and the free-stream flow velocity was set to U_∞=20 m/s. The detailed locations of the measurements are shown in Fig. 2. The locations are denoted by BL_1, BL_2, BL_3 and BL_4. The distance between the two neighbouring lines corresponds to 1/3L_{px}. The hot-wire probe has been traversed and the data has been collected between $y \approx 0\ mm$ and y = 50 mm at 35 points above the plate for each line.

Figure 3 presents the mean and rms boundary layer velocity profiles along the BL lines shown in Fig. 2. The y axis of the boundary layer profile have been normalized by the boundary layer thickness at BL_1. Note that at BL_1, the velocity of fluid goes to zero at the boundary in which that the no-slip condition is still valid at the wall and is not the same in the case of porous boundary. The velocity profile results for both solid and porous cases show that there is an increase in the velocity gradient at the wall from BL_1 to BL_4 and the boundary layer thickness found to be decreasing from BL_2 to BL_4. This implies that favorable or negative pressure gradient occurs near the TE which tend to accelerate the flow [17]. All of the boundary layer profiles downstream of BL_1 change for all cases, as the bluntness causes significant velocity overshoot in the vicinity of the trailing edge. Results have shown that the porous materials decrease the bluntness acceleration, *i.e.* the red and blue profiles show

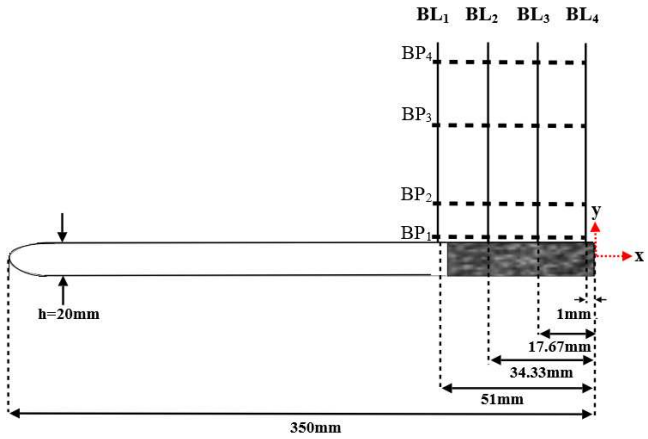

Figure 2: The schematic of the blunt trailing edge rig and the positions of the hot-wire measurements

lower velocities. The 25 PPI material reduces the acceleration the most, which is well visible at the BL_4 location.

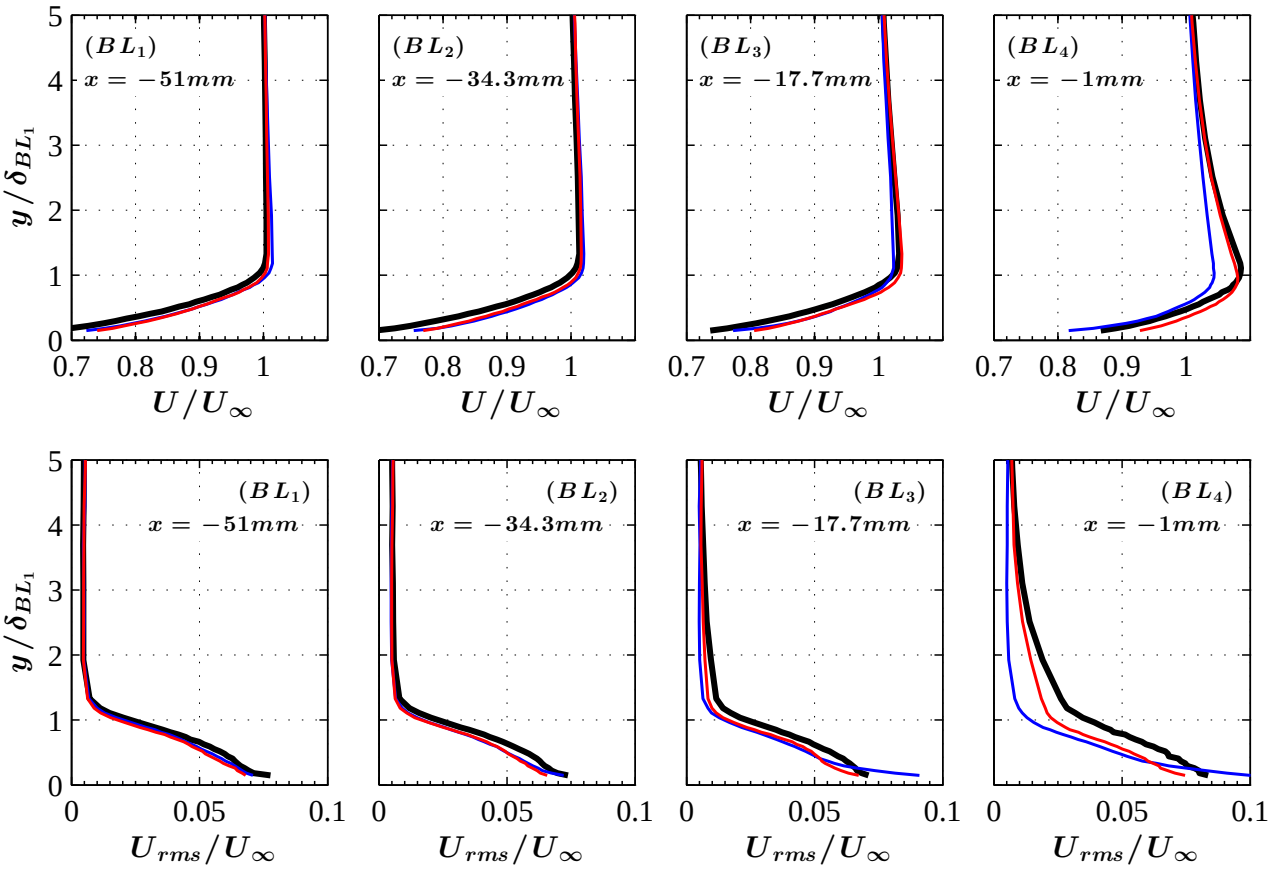

Figure 3: Boundary layer mean and RMS velocity profiles at different streamwise locations over the blunt trailing edge flat plate model. *black line: solid; blue line: porous 25 PPI; red line: porous 80 PPI.*

The presented RMS velocity profiles show reduction when the porous material was applied at the trailing edge. This becomes clearly visible at x=17.7mm (BL_3) and x=1mm (BL_4), upstream of the trailing edge. However, there is an increase in the RMS velocity magnitude near the wall especially

for the case of porous 25 PPI at both BL_3 and BL_4. This means that there is an increase in the energy content near the wall, which is believed to have been caused due to viscous friction effect taken place at the porous surface. However, results show that the overall energy content in the boundary layer is significantly reduced by both porous materials, especially by the 25 PPI one.

3.2 Velocity Power Spectra in the Boundary Layer

The location of the dominant turbulent structures within the boundary layer and their frequency energy content can be studied using the velocity power spectrum (ϕ_{uu}). Figure 4 presents the velocity power spectral density as a function of the Strouhal number at different axial locations upstream of the TE and provides comparison between the three investigated cases. The spectra at BP_{1-3}, BL_{1-4} shows the near wall region, of which BP_1 correspond to the point near the surface. The spectra at BP_4, BL_{1-4}, on the other hand, show the outer layer of the boundary layer. In the vicinity of the wall, the porous material especially in the case of 25 PPI causes an increase in the energy content over the whole Strouhal range, which is in agreement with the RMS velocity profiles in Fig. 3.

The investigated spectra at BP_3, BL_{1-4} corresponds to the inner edge of the turbulent boundary layer. At these locations, it is clearly visible that the energy content of the porous cases have been reduced significantly. However, in the outer layer (BP_4, BL_{1-4}), all the porous materials experience an increase in the energy content compared to the solid TE, which appears to be due to the detached eddies from the TE wall. The inner layer is predominantly composed of wall attached eddies of quasi-streamwise vortices. The characteristics between attached and detached eddies are given by Perry and Marušic [18]. Consequently, these eddies in the inner layer, which interacts on the TE wall, will have a very significant effect on their structure. The energy reduction observed in the case of porous TE is believed to be the result of eddies break-up in the porous media. The tonal peaks are well visible for solid and porous 80 PPI in the vicinity of the TE at BL_{3-4}. The tonal peak occurs at $St \approx 0.21$, which corresponds to the vortex shedding frequency as expected. The peaks vanish in the case of the 25 PPI porous material apart from the BP_4, BL_4 (upper right plot) case. This is believed to be due to the fact that this material has a flow stabilizing effect in the near wake regions.

3.3 Surface Pressure Measurement

In characterizing the noise generated from the trailing edge, it is essential to examine both the fluid field and the pressure exerted on the surface. The correlation studies between the velocity field within the BL and the surface pressure fluctuations were conducted in order to identify the characteristics of the coherent turbulent structure and the statistical properties of fluctuations in space and phase relation. The flow velocity was set to U_∞=20 m/s and the measurements were taken at four locations above the microphones numbered 1,2,4 and 6. The locations are denoted by BL_{m1}, BL_{m2}, BL_{m4} and BL_{m6}. Cross-wire probe has been used and the data has been collected between $y \approx 0\ mm$ and y = 50 mm at 49 locations above each microphone.

Figure 5 presents the velocity-pressure $R_{u'p'}$ and $R_{v'p'}$ correlation profiles within the BL at different distances from the trailing edge. Two point correlation function of the velocity ($R_{ii}(r)$=$< u_i'(x_i,t)u_i'(x_i+r,t) > / < (u_i')^2 >$) was used to compute the results. The y axis of the velocity-pressure correlation plots have been normalized by the boundary layer thickness at BL_1 (Fig. 2). It is noticed that the values of correlation coefficient clearly increase in the negative scale downstream of the trailing edge for all porous cases in both $R_{u'p'}$ and $R_{v'p'}$ correlation profiles at the locations near to the wall. As for the solid case, the $R_{u'p'}$ correlation is highly concentrated in the negative region at the positions closer to the wall between BL_{m1} to BL_{m4}, and positively correlated at BL_{m6}. The positive correlation can also be seen for the case of porous 80 PPI at the locations $y/\delta_{BL_1} > 2$, *i.e.* at BL_{m3} and BL_{m4}, however this trend does not appear in the case of porous 25 PPI. On the contrary, the $R_{v'p'}$ value is negatively correlated for all cases, where porous 80 PPI displays higher correlation value compared to others. Taylor [19] interpreted that the negative correlation is believed to occur

due to some sort of regularity which exist in the eddies motion. The negative correlation in Fig. 5 also indicates that an increase in the velocity or pressure fluctuating signal reliably predicts a decrease in the other one. In other words, the negative correlation demonstrate that the fluctuating velocity components ($u^{'}$, $v^{'}$) and $p^{'}$ are out of phase in the flow. The change of these components phase is believed to have been caused due to the flow acceleration at the trailing edge, which is in agreement with the results obtained in Fig. 3.

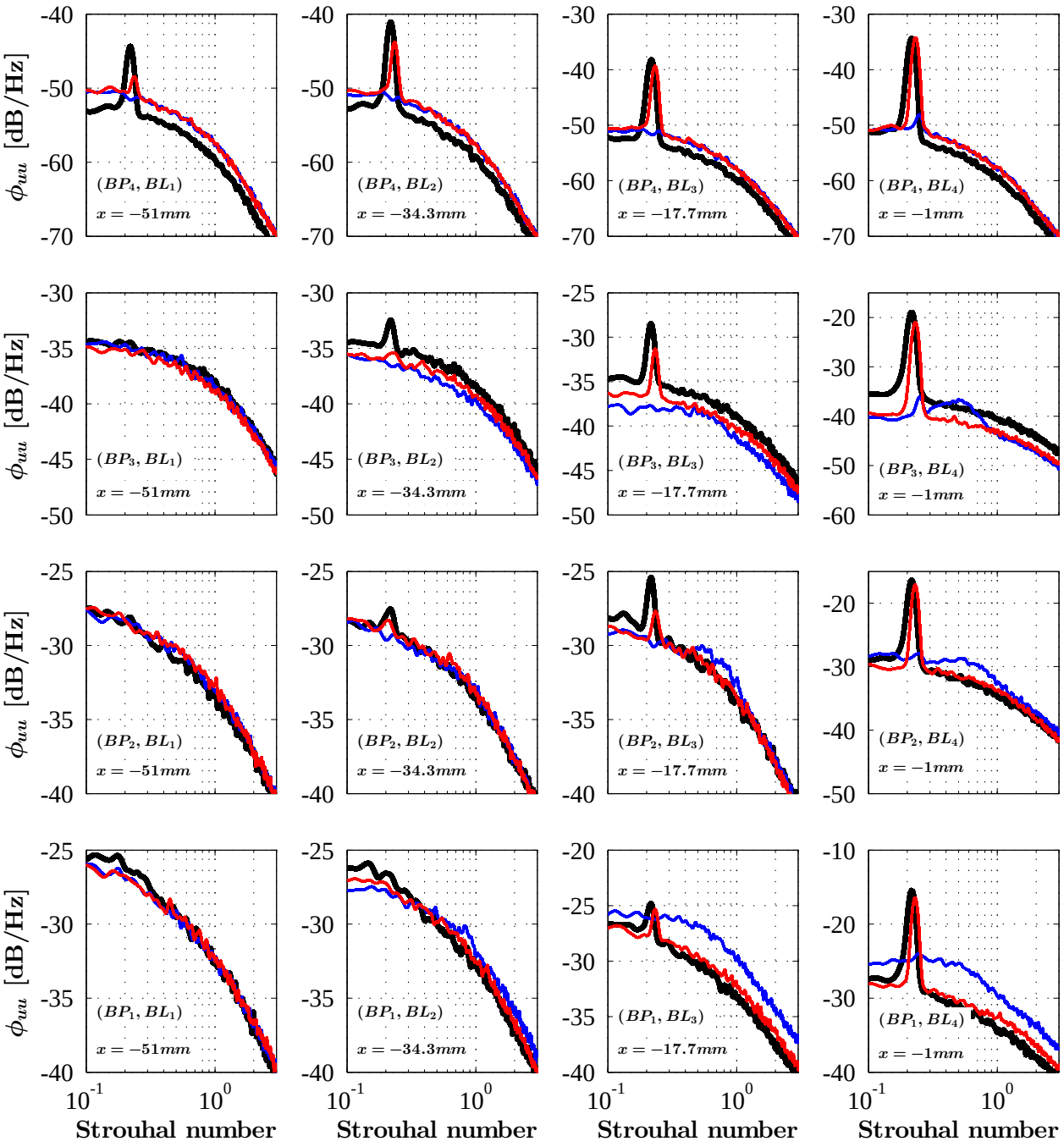

Figure 4: The power spectral density at different locations in the boundary layer. *black line: solid; blue line: porous 25 PPI; red line: porous 80 PPI*

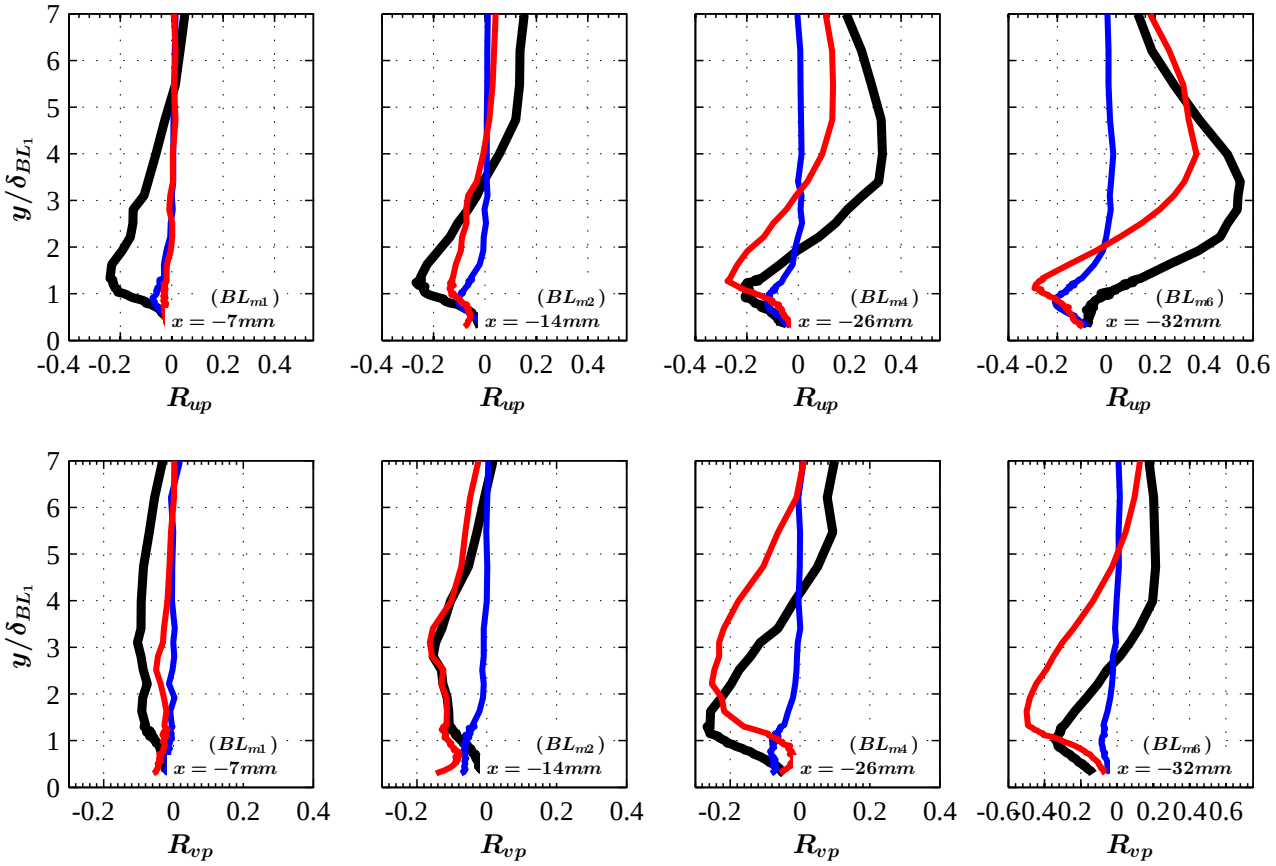

Figure 5: Velocity-Pressure Correlation, $R_{u'p'}$ (upper row) and $R_{v'p'}$ (lower row) in the Boundary Layer correlation profiles at different streamwise locations over the blunt trailing edge. *black line: solid; blue line: porous 25 PPI; red line: porous 80 PPI.*

4. Conclusion

The aerodynamics and aeroacoustics of the flow around a blunt trailing edge has been addressed and several measurements have been carried out in the open jet wind tunnel of the University of Bristol. The effect of applying porous treatments at the trailing edge have been widely investigated by single and cross hot-wire measurements and boundary layer surface pressure measurements. It was found that porous materials are capable of reducing the acceleration of the flow in the boundary layer upstream of the trailing edge. The power spectra results showed that significant reduction was achieved in the outer layer of the boundary layer. It is also obvious that the porous treatment has noticeably modified the velocity-pressure correlation in the boundary layer. Thus, it is evident that the porous treatment significantly improved the aerodynamic performance and weakened the noise generation mechanism for the trailing edge bluntness flow.

5. Acknowledgement

This project is sponsored by Embraer S.A. . The second author (MA) would like to acknowledge the financial support of the Royal Academy of Engineering.

References

1. Lyu, B., Azarpeyvand, M. and Sinayoko, S. Prediction of noise from serrated trailing edges, *Journal of Fluid Mechanics*, **793**, 556–588, (2016).

2. Gruber, M., Azarpeyvand, M. and Joseph, P. F. Airfoil trailing edge noise reduction by the introduction of sawtooth and slitted trailing edge geometries, *integration*, **10**, 6, (2010).

3. Azarpeyvand, M., Gruber, M. and Joseph, P. F. An analytical investigation of trailing edge noise reduction using novel serrations, *19th AIAA/CEAS Aeroacoustic Conference*, pp. 27–29, (2013).

4. Sinayoko, S., Azarpeyvand, M. and Lyu, B. Trailing edge noise prediction for rotating serrated blades, *20th AIAA/CEAS Aeroacoustics Conference*, pp. 16–20, (2014).

5. Liu, X., Azarpeyvand, M. and Theunissen, R. Aerodynamic and aeroacoustic performance of serrated airfoils, *21st AIAA/CEAS Aeroacoustics Conference*, p. 2201, (2015).

6. Ai, Q., Azarpeyvand, M., Lachenal, X. and Weaver, P. M. Aerodynamic and aeroacoustic performance of airfoils with morphing structures, *Wind Energy*, (2015).

7. Ai, Q., Weaver, P. and Azarpeyvand, M. Design optimization of a morphing flap device using variable stiffness materials, *24th AIAA/AHS Adaptive Structures Conference*, p. 0816, (2016).

8. Liu, H., Azarpeyvand, M., Wei, J. and Qu, Z. Tandem cylinder aerodynamic sound control using porous coating, *Journal of Sound and Vibration*, **334**, 190–201, (2015).

9. KJ., S. and van Dam CP. Aerodynamic analysis of blunt trailing edge airfoils, *Journal of Solar Energy Engineering | Volume 125 | Issue 4 | TECHNICAL PAPERS*, (2003).

10. Hoerner, S. F. and Borst, H. V. Fluid-dynamic lift: practical information on aerodynamic and hydrodynamic lift, (1985).

11. Bae, Y., Jeong, Y. E. and Moon, Y. J. Effect of porous surface on the flat plate self-noise, *Proceedings of the 15th AIAA/CEAS Aeroacoustics Conference, AIAA-Paper*, no. 2009-3311, (2009).

12. Bae, Y. and Moon, Y. J. Effect of passive porous surface on the trailing-edge noise, *Physics of Fluids (1994-present)*, **23** (12), 126101, (2011).

13. Zhou, B. Y., Gauger, N. R., Koh, S. R., Meinke, M. and Schröder, W. Adjoint-based trailing-edge noise minimization using porous material.

14. Rae, W. H. and Pope, A., *Low-speed wind tunnel testing*, John Wiley (1984).

15. Bull, M. and Thomas, A. High frequency wall-pressure fluctuations in turbulent boundary layers, *Physics of Fluids (1958-1988)*, **19** (4), 597–599, (1976).

16. Bull, M. Wall-pressure fluctuations beneath turbulent boundary layers: some reflections on forty years of research, *Journal of Sound and Vibration*, **190** (3), 299–315, (1996).

17. AKERNATHY, F. H. Fundamentals of boundary layers, (1988).

18. Perry, A. and Marušic, I. A wall-wake model for the turbulence structure of boundary layers. part 1. extension of the attached eddy hypothesis, *Journal of Fluid Mechanics*, **298**, 361–388, (1995).

19. Taylor, G. I. Diffusion by continuous movements, *Proc. London Math. Soc*, **20** (1), 196–212, (1922).